Available online at www.sciencedirect.com

ScienceDirect

IFAC Papers Online CONFERENCE PAPER ARCHIVE

IFAC-PapersOnLine 49-26 (2016) 318–323

Dynamic metabolic flux analysis of underdetermined and overdetermined metabolic networks

Sofia Fernandes * **Julien Robitaille** *** **Georges Bastin** ** **Mario Jolicoeur** *** **Alain Vande Wouwer** *

* *Automatic Control Laboratory, University of Mons, 31 Boulevard Dolez, 7000 Mons, Belgium (e-mail: sofia.afonsofernandes and alain.vandewouwer@umons.ac.be)*

** *Université catholique de Louvain, ICTEAM, Department of Mathematical Engineering, av. G. Lemaitre 4, B1348 Louvain-La-Neuve, Belgium (e-mail: Georges.Bastin@uclouvain.be)*

*** *Laboratory in Applied Metabolic Engineering, Department of Chemical Engineering, École Polytechnique de Montréal, C.P. 6079, Centre-ville Station, Montréal(Quebec), Canada (e-mail: Julien.Robitaille@nrc-cnrc.gc.ca and mario.jolicoeur@polymtl.ca)*

Abstract: In this work, two metabolic networks representing the metabolism of CHO cells in fed-batch cultures are considered. The first metabolic network is relatively detailed and underdetermined with the available extracellular measurements, while the second is a reduced version of the former and is overdetermined. A dynamic metabolic flux analysis based on convex analysis (DMFCA) is applied to the detailed network, which allows the computation of the time evolution of bounded intervals. On the other hand, a linear optimization problem is solved for the reduced-size network, with either positivity constraints or box constraints inferred from DMFCA. In all cases, smoothing splines and mass balance differential equations are used to infer the time evolution of the uptake and excretion rates from experimental data. The analysis allows to get insight into CHO metabolism as well as to investigate the influence of the size of the metabolic network.

Keywords: CHO cells, Dynamic metabolic flux analysis, Convex analysis, Underdetermined system, Overdetermined system, linear optimization.

1. INTRODUCTION

Metabolic flux analysis (MFA) is a useful tool to determine intracellular fluxes from extracellular measurements, such as cell density, substrates and products concentrations in, among others, mammalian cell cultures. Determining in vivo fluxes provides quantitative information on the degree of engagement of various metabolic pathways in the overall cellular metabolism. The classical MFA method is used to study systems at metabolic steady state, meaning that intracellular fluxes do not change in time. This assumption is supported by the observation that intracellular dynamics are much faster than extracellular dynamics (Stephanopoulos et al., 1998). This assumption is usually applied during the early exponential growth in batch cultures and in steady-state continuous cultures (Niklas et al., 2011). However, classical MFA does not provide information on metabolic transient. To overcome this weakness, the development of dynamic metabolic flux analysis (DMFA) techniques has been addressed (Leighty and Antoniewicz, 2011; Lequeux et al., 2010; Llaneras et al., 2012; Vercammen et al., 2014; Robitaille et al., 2015; Fernandes de Sousa et al., 2015).

A particular aspect of MFA is that depending on the information provided by extracellular measurements and on the properties of the stoichiometric matrix, the system can be determined, overdetermined or underdetermined.

In this study, two metabolic networks are considered in order to understand CHO metabolism as well as to discuss the importance of the size of the metabolic network. To this end, an underdetermined and an overdetermined metabolic networks are considered. Basically, these metabolic networks embrace the same major metabolic pathways: glycolysis, pentose phosphate pathway, TCA cycle, amino acids metabolism, nucleotides, biomass and antibody synthesis. The small-size network can be obtained by reduction of the larger, more detailed network. Of course, there is no exact metabolic network to represent cellular metabolism: a candidate metabolic network is based on available metabolic knowledge and built in a way that allows describing the consumption and production of the available extracellular metabolites in a satisfactory manner. Special care has to be exercised to preserve the stoichiometry while lumping and/or combining reactions.

To obtain the flux distribution in the larger metabolic network, a dynamic metabolic flux analysis using convex analysis (Fernandes de Sousa et al., 2015) is applied. DMFCA is an approach suitable for underdetermined

2405-8963
Peer review under responsibility of International Federation of Automatic Control.
10.1016/j.ifacol.2016.12.146

systems, and does not require the definition of ad-hoc objective functions. Mass balance differential equations for the extracellular concentrations, together with cubic spline smoothing, are used to assess the time evolution of the uptake and excretion rates. This information is then processed by convex analysis assuming that the intracellular species are in pseudo-steady state with respect to the time evolution of the extracellular concentrations (slow-fast approximation). This method allows determining bounded intervals for each intracellular flux, and makes the most of the available information (metabolic network and available extracellular measurements) without introducing additional constraints or objective function.

The flux distribution in the reduced-size network is determined by solving a linear optimization problem using Linear Programming (LP). The problem is first solved under positivity constraints, which is the basic assumption when no additional a priori information is available. Then, the problem is solved under box constraints inspired by the bounded intervals obtained by DMFCA.

Both DMFCA and LP methods are applied to experimental data collected from CHO fed-batch cultures.

This paper is organized as follows. The next section describes briefly the experimental data. Both metabolic networks are introduced in section 3. In section 4, the DMFCA problem is formulated, including extracellular dynamic mass balance equations, spline smoothing of the experimental data, and determination of bounded intervals for the intracellular fluxes using convex analysis. The linear optimization problem is formulated in section 5. Section 6 is devoted to the numerical results and section 7 draws some conclusions.

2. EXPERIMENTAL DATA

Our study is based on a set of experimental data from fed-batch cultures of CHO-DXB11 cell line, producing a chimeric heavy chain monoclonal antibody (EG2-hFc) (Robitaille et al., 2015). This set contains the time evolution of the extracellular concentrations of biomass, recombinant mAb, glucose, glutamine, lactate, alanine, ammonia and 15 amino acids (except leucine, tryptophan and cysteine). The fed-batch culture was fed daily with punctual injections of fresh medium, to avoid nutrients limitation (see figure 1). Mathematically speaking, this type of fed-batch, with punctual injections, can be considered as a succession of batch cultures with different initial conditions.

For more details about the experimental procedure and analytical methods, the reader is referred to (Robitaille et al., 2015).

3. METABOLIC NETWORK

Two metabolic networks are considered in this work. The first one is relatively detailed (see table 2) and contains 72 biochemical reactions, 45 internal metabolites and 21 extracellular metabolites present in the culture medium, which are either substrates or products. The second one is described in (Robitaille et al., 2015) and contains 29 reactions, 16 internal metabolites and 21 extracellular measurements. Both metabolic networks embrace the major reactions of central metabolism such as glycolysis, Tricarboxylic Cycle Acid (TCA), Penthose Phosphate Pathway (PPP) and amino acids metabolism. Biomass and antibody synthesis are also incorporated into the model. The stoichiometric coefficients of the biomass and antibody synthesis were taken from literature (Robitaille et al., 2015). The small-size network can be obtained by reduction of the larger network. If N_u and N_o are the stoichiometric matrices of the underdetermined and overdetermined networks, respectively, it is possible to prove that $N_o \in N_u$, through the following steps:

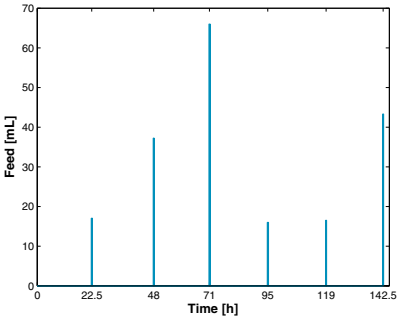

Fig. 1. Feeding strategy over CHO-DXB11 fed-batch culture.

- Reactions v_3 and v_4 are lumped into an overall reaction.
- Reactions v_{10} and v_{11} are lumped into an overall reaction and the metabolite Succinyl-CoenzymeA (SucCoA) is eliminated.
- Reactions v_{12} and v_{13} are lumped into an overall reaction and the metabolite Fumarate (Fum) is eliminated.
- Reactions v_{30}, v_{31}, v_{32}, v_{33}, v_{34}, v_{35}, v_{36}, v_{37} and v_{39} are lumped into an overall reaction (this reaction is called amino acids transamination in Robitaille's work).
- According to Robitaille's work, the amino acids threonine, phenylalanine, methionine and cysteine are only used to biomass and mAb synthesis. Therefore, reactions v_{25}, v_{38}, v_{40} and v_{41} are not taken into account.
- Reactions v_{43}, v_{44}, v_{45}, v_{46} and v_{47} are lumped into an overall reaction (in Robitaille's work, this reaction is called Histidine/arginine transamination).
- Reactions v_{26}, v_{27}, v_{28}, v_{48}, v_{49} and v_{50} are not taken into account in Robitaille's network.
- The only transport reaction considered in Robitaille's work is the one of glutamate (Glu).

Table 2. Metabolic network of CHO cells.

Flux	Reactions
	Glycolysis
v_1	$Glc_{ext} + ATP \rightarrow G6P + ADP$
v_2	$G6P \leftrightarrow F6P$

Flux	Reactions
v_3	$F6P + ATP \rightarrow DHAP + G3P + ADP$
v_4	$DHAP \leftrightarrow G3P$
v_5	$G3P + NAD^+ + ADP \leftrightarrow 3PG + NADH + ATP$
v_6	$3PG + ADP \rightarrow Pyr + ATP$
	Tricarboxylic Acid Cycle
v_7	$Pyr + NAD^+ + CoASH \rightarrow AcCoA + CO_2 + NADH$
v_8	$AcCoA + Oxal + H_2O \rightarrow Cit + CoASH$
v_9	$Cit + NAD(P)^+ \rightarrow \alpha KG + CO_2 + NAD(P)H$
v_{10}	$\alpha KG + CoASH + NAD^+ \rightarrow SucCoA + CO_2 + NADH$
v_{11}	$SucCoA + GDP + Pi \leftrightarrow Succ + GTP + CoASH$
v_{12}	$Succ + FAD \leftrightarrow Fum + FADH_2$
v_{13}	$Fum \leftrightarrow Mal$
v_{14}	$Mal + NAD^+ \leftrightarrow Oxal + NADH$
	Pyruvate Fates
v_{15}	$Pyr + NADH \leftrightarrow Lac_{ext} + NAD^+$
v_{16}	$Pyr + Glu \leftrightarrow Ala + \alpha KG$
	Pentose Phosphate Pathway
v_{17}	$G6P + 2NADP^+ + H_2O \rightarrow R5P + 2NADPH + CO_2$
v_{18}	$R5P \leftrightarrow X5P$
v_{19}	$2X5P + R5P \leftrightarrow 2F6P + G3P$
	Anaplerotic Reaction
v_{20}	$Pyr + ATP \rightarrow Oxa + ADP$
v_{21}	$Mal + NAD(P)^+ \leftrightarrow Pyr + CO_2 + NAD(P)H$
	Amino Acid Metabolism
v_{22}	$Glu + NAD(P)^+ \leftrightarrow \alpha KG + NH_4^+ + NAD(P)H$
v_{23}	$Oxal + Glu \leftrightarrow Asp + \alpha KG$
v_{24}	$Gln \rightarrow Glu + NH_4^+$
v_{25}	$Thr + NAD^+ + CoASH \rightarrow Gly + NADH + AcCoA$
v_{26}	$Ser \leftrightarrow Gly$
v_{27}	$3PG + Glu + NAD^+ \rightarrow Ser + \alpha KG + NADH$
v_{28}	$Gly + NAD^+ \rightarrow CO_2 + NH_4^+ + NADH$
v_{29}	$Ser \rightarrow Pyr + NH_4^+$
v_{30}	$\alpha Kb + CoASH + NAD^+ \rightarrow PropCoA + NADH + CO_2$
v_{31}	$PropCoA + HCO_3^- + ATP \rightarrow SucCoA + ADP + Pi$
v_{32}	$Lys + 2\alpha KG + 3NAD(P) + FAD^+ \rightarrow \alpha Ka + 2Glu + 3NAPH + FADH_2$
v_{33}	$\alpha Ka + CoASH + 2NAD^+ \rightarrow AcetoAcCoA + 2NADH + 2CO_2$
v_{34}	$AcetoAcCoA + CoASH \rightarrow 2AcCoA$
v_{35}	$Val + \alpha KG + CoASH + 3NAD^+ + FAD^+ \rightarrow PropCoA + Glu + 2CO_2 + 3NADH + FADH_2$
v_{36}	$Ile + \alpha KG + 2CoASH + 2NAD^+ + FAD^+ \rightarrow AcCoA + Glu + CO_2 + 2NADH + FADH_2 + PropCoA$
v_{37}	$AcetoAc + SucCoA \rightarrow AcetoAcCoA + Succ$
v_{38}	$Phe + NADH \rightarrow Tyr + NAD^+$
v_{39}	$Tyr + \alpha KG \rightarrow Fum + AcetoAc + Glu + CO_2$
v_{40}	$Met + Ser + ATP \rightarrow Cys + \alpha Kb + NH_4^+ + AMP$
v_{41}	$Cys \rightarrow Pyr + NH_4^+$
v_{42}	$Asn \leftrightarrow Asp + NH_4^+$
v_{43}	$Arg \rightarrow Orn + urea$
v_{44}	$Orn + \alpha KG \leftrightarrow Glu\gamma SA + Glu$
v_{45}	$Pro \rightarrow Glu\gamma SA$
v_{46}	$Glu\gamma SA + NAD(P)^+ \rightarrow Glu + NAD(P)H$
v_{47}	$His \rightarrow Glu + NH_4^+$
v_{48}	$Orn + CarbP \rightarrow Cln$
v_{49}	$Cln + Asp + ATP \rightarrow ArgSucc + AMP$
v_{50}	$ArgSucc \rightarrow Arg + Fum$
	Nucleotide Synthesis
v_{51}	$0.6R5P + 2Gln + 2Asp + Gly + CO_2 + 2ATP \rightarrow 2Glu + 2MAL + AMP + 2ADP$
	Biomass Synthesis
v_{52}	$0.06Ala + 0.04Arg + 0.04Asn + 0.03Asp + 0.02Gln + 0.04Glu + 0.06Gly + 0.02His + 0.09Ile + 0.06Lys + 0.01Met + 0.02Phe + 0.03Pro + 0.05Ser + 0.04Thr + 0.02Tyr + 0.04Val + 3.78ATP + 0.03G6P + 0.03R5P + 0.09Cit \rightarrow Biomass + 3.78ADP$
	Antibody Synthesis
v_{53}	$0.06Ala + 0.02Arg + 0.05Asn + 0.04Asp + 0.04Gln + 0.05Glu + 0.07Gly + 0.02His + 0.10Ile + 0.06Lys + 0.01Met + 0.04Phe + 0.07Pro + 0.11Ser + 0.11Thr + 0.03Tyr + 0.09Val + 4ATP \rightarrow mAb + 3.78ADP$
	Transport Reactions
v_{54}	$Asp_{ext} \rightarrow Asp$
v_{55}	$Asn_{ext} \rightarrow Asn$
v_{56}	$Gly \rightarrow Gly_{ext}$
v_{57}	$Ser_{ext} \rightarrow Ser$
v_{58}	$Glu \rightarrow Glu_{ext}$
v_{59}	$Tyr_{ext} \rightarrow Tyr$
v_{60}	$Ala \rightarrow Ala_{ext}$
v_{61}	$Arg_{ext} \rightarrow Arg$
v_{62}	$Gln_{ext} \rightarrow Gln$
v_{63}	$His_{ext} \rightarrow His$
v_{64}	$Ile_{ext} \rightarrow Ile$
v_{65}	$Lys_{ext} \rightarrow Lys$
v_{66}	$Met_{ext} \rightarrow Met$
v_{67}	$Phe_{ext} \rightarrow Phe$
v_{68}	$Thr_{ext} \rightarrow Thr$
v_{69}	$Val_{ext} \rightarrow Val$
v_{70}	$NH_4^+ \rightarrow NH_{4\ ext}^+$
v_{71}	$Pro_{ext} \rightarrow Pro$
v_{72}	$CO_2 \rightarrow CO_{2ext}$

4. UNDERDETERMINED NETWORK

To solve the underdetermined system, Dynamic Metabolic Flux Convex Analysis (Fernandes de Sousa et al., 2015) is used.

4.1 Dynamic Metabolic Flux Convex Analysis

The goal of DMFCA is to compute a set of admissible flux distributions continuously over time $v(t)$, using a pseudo-steady state assumption (no accumulation of internal metabolites):

$$\begin{pmatrix} N_i^{45\times 72} & 0 \\ N_m^{21\times 72} & -v_m^{21\times 1}(t) \end{pmatrix} \times \begin{pmatrix} v(t) \\ 1 \end{pmatrix} = 0 \qquad (1)$$

where N_i is the stoichiometric matrix deduced from the metabolic network, N_m is the matrix connecting the fluxes to the available measurements and v_m represents the specific uptake and excretion rates of the measured extracellular species.

The metabolic network under study is not redundant ($rank(N_i) = m = 45$), and with the information provided by 21 extracellular measurements, it is an underdetermined system with a degree of freedom of 6.

Extracellular flux determination Extracellular fluxes of the twenty-one metabolites can be computed based on their mass balance differential equations, involving cellular growth (μ), substrate uptake (υ_s) and product secretion (υ_p), as described by:

$$\frac{dX}{dt} = (\mu - D)X \qquad (2)$$

$$\frac{dS}{dt} = -DS - \upsilon_s X + DS_{in} \qquad (3)$$

$$\frac{dP}{dt} = -DP + \upsilon_p X + DP_{in} \qquad (4)$$

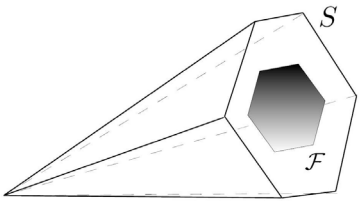

Fig. 2. Convex polyedron cones S and $\mathcal{F}$.

where X, S, P, S_{in}, P_{in} and D denote biomass, substrate, product, influent substrate and product and dilution rate, respectively. The dilution rate is defined as $D = \frac{F_{in}}{V}$, where F_{in} is the inlet feed rate and V the broth volume.

Firstly, the experimental data is smoothed off using smoothing splines and then the time derivatives appearing on the left-hand side of equations 2-4 are evaluated.

Intracellular flux determination The set of solutions to equation 1 can be computed using convex analysis. This approach is based on the interpretation of elementary fluxes modes (simplest metabolic pathways linking substrates to products) and makes the most of the available information (i.e., metabolic network and extracellular measurements) without imposing any artificial constraint.

Geometrically speaking, the set of positive solutions to $N_i v(t) = 0$ generates a convex polyhedron cone S (see figure 2). Any flux distribution v in the cone S can be expressed as a non-negative linear combination of a set of elementary flux vectors e_i, which are the edges of the polyhedral cone S:

$$v(t) = w_1(t)e_1(t)+w_2(t)e_2(t)+\cdots+w_p(t)e_p(t), \qquad w_i(t) \geq 0 \tag{5}$$

If the system is further constrained with the information provided by the extracellular measurements (specific uptake and excretion rates), the solution space reduces to a convex polytope $\mathcal{F}$ in the positive orthant, where each admissible flux distribution $v(t)$ can be expressed as a convex combination of a set of non-negative basis vectors f_i which are the edges of this polytope. The set of admissible flux vectors is defined as:

$$v(t) = \sum_i w_i(t) f_i(t), \qquad w_i(t) \geq 0, \qquad \sum_i w_i(t) = 1 \tag{6}$$

The basis vectors $f_i(t)$, the so-called elementary flux vectors of the flux space $\mathcal{F}$, can be obtained applying the software METATOOL (Pfeiffer et al., 1999) or EFMTool (Terzer and Stelling, 2008) to the matrix:

$$\begin{pmatrix} N_i^{45\times 72} & 0 \\ N_m^{21\times 72} & -v_m^{21\times 1}(t) \end{pmatrix} \tag{7}$$

and in turn the admissible bounds $v_j^{min}(t)$ and $v_j^{max}(t)$ for each admissible flux $v_j(t)$:

$$\begin{aligned} &v_j^{min}(t) \leq v_j(t) \leq v_j^{max}(t), \\ &\quad with \\ &v_j^{min}(t) = \min_i f_i^j(t), v_j^{max}(t) = \max_i f_i^j(t) \end{aligned} \tag{8}$$

where $f_i^j(t)$ is the j-th component of the i-th basis vector $f_i(t)$. Note that METATOOL calculates 13 7063 elementary flux modes from the set of positive solutions $N_i v(t) = 0$. However, after the system being constrained with the information provided by the extracellular measurements, the number of elementary flux vectors decreases drastically. For example, at $t = 0$ only 80 elementary flux vectors are computed.

The system is said well posed if the solution set is not empty and if all the metabolic fluxes are bounded. Otherwise, the system is said to be ill posed and additional extracellular information has to be provided.

5. OVERDETERMINED SYSTEM

The linear system of equations to solve in the least squares sense is given by:

$$\begin{pmatrix} N_{i_{small}}^{16\times 29} \\ N_{m_{small}}^{21\times 29} \end{pmatrix} \times v(t)^{37\times 1} = \begin{pmatrix} 0 \\ v_m^{21\times 1}(t) \end{pmatrix} \tag{9}$$

where $N_{i_{small}}$ and $N_{m_{small}}$ are the stoichiometric matrices of the reduced-size network, connecting the fluxes to the internal metabolites and to the available measurements, respectively.

At first, it is assumed that the fluxes are positive:

$$v(t) \geq 0 \tag{10}$$

which is the only a priori knowledge.

In a further step, the linear optimization problem can be solved under box constraints:

$$v_{min}(t) \leq v(t) \leq v_{max}(t) \tag{11}$$

where v_{min} and v_{max} are lower and upper bounds, which can be inferred from DMFCA.

The Matlab function lsqlin is used as the optimization tool to solve problem 9-10 or problem 9-11. The application of this algorithm allows the definition of a relative error in the measurement vector (v_m). In this study, a relative error of 5% is assumed (which is obviously an approximate value, as it takes into account of the experimental errors but also of the data processing to estimate the uptake and excretion rates).

6. NUMERICAL RESULTS

Based on the previous metabolic networks, DMFCA and LP are applied to experimental data from CHO fed-batch cultures in order to get insight into the flux distribution and assess the influence of the construction of the metabolic network. Recombinant mAb, glucose, glutamine, lactate, alanine, ammonia and 15 amino acids (except leucine, tryptophan and cysteine) are the available extracellular experimental data.

6.1 Glycolysis and Pentose phosphate pathways

The PPP is present in the cytosol of all cells and has two major functions: (1) to synthesize ribose 5-phosphate, which is required for nucleotide and nucleic acid synthesis; and (2) reducing power in the form of NADPH. PPP also provides an alternative pathway for glucose oxidation. However, in most tissues, 80-90% of glucose oxidation is via glycolysis and the remaining 10-20% occurs via PPP (Wamelink et al., 2008). Also, several studies have demonstrated that the G6P is mostly converted to pyruvate by glycolysis and in less quantities by PPP either in hybridoma or CHO cells (Ahn and Antoniewicz, 2011; Sengupta et al., 2011). Indeed, in this study, comparing metabolic fluxes v_2 and v_{17}, obtained using LP with positivity constraints or with box constraints, one can observe that conversion of G6P to pyruvate by PPP is very low when compared to glycolysis (figure 3). This observation is not clear when comparing both fluxes v_2 and v_{17} obtained by DMFCA. This is explained by the fact that Glycolysis and PPP are set in parallel, and thus are not distinguishable applying DMFCA from extracellular measurements only. The assimilation of G6P could occur in the Glycolysis or in the PPP indistinctly, and thus their flux intervals are in counterbalance.

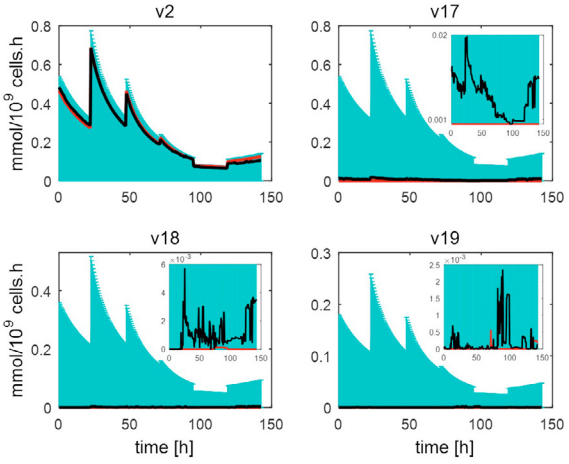

Fig. 3. Dynamic evolution of Glycolysis (v_2) and PPP (v_{17}-v_{19}) metabolic fluxes along time culture. Turquoise: DMFCA. Black: LP with positivity constraint. Red: LP with DMFCA constraints.

6.2 Anaplerotic Reactions

The anaplerotic reactions are known to be important for the replenishment of TCA cycle intermediates. In this study, two anaplerotic reactions are considered: the pyruvate carboxylase (v_{20}) and the malic enzyme (v_{21}). From figure 4 one can see that the flux of malic enzyme is higher than the flux of pyruvate carboxylase when DMFCA constraints are considered. The higher efflux of malate out of TCA cycle implies a higher rate for its conversion to pyruvate. In turn, pyruvate can be used to enter in TCA cycle via Acetyl-CoA, to produce lactate or to participate in the synthesis of alanine. As shown in figure 5, in most of the culture, the majority of the pyruvate is channeled mainly towards lactate (see figure 6). The inefficient use of glucose for ATP production is a well known characteristic of CHO cells - phenomenon characterized as Warburg effect (Vazquez et al., 2010), where most of the available glucose is converted into lactate obtaining ATP from an aerobic glycolysis process.

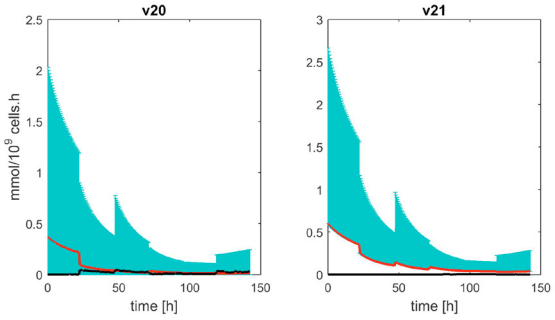

Fig. 4. Dynamic evolution of anaplerotic reactions along time culture. Turquoise: DMFCA. Black: LP with positivity constraint. Red: LP with DMFCA constraints.

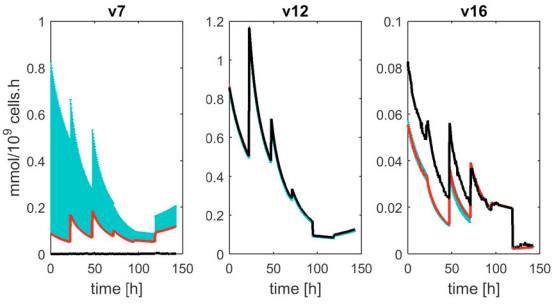

Fig. 5. Dynamic evolution of pyruvate fates along time culture. Turquoise: DMFCA. Black: LP with positivity constraint. Red: LP with DMFCA constraints.

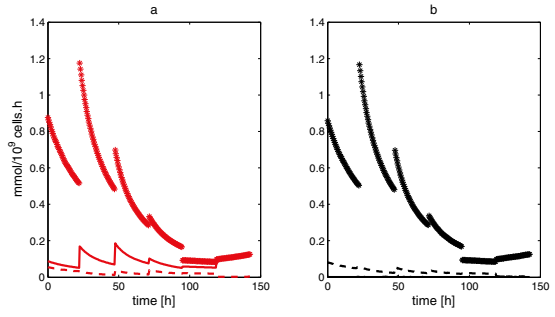

Fig. 6. Comparison between pyruvate fates. For **a** and **b**. asterisk: Pyruvate producing lactate (v_{15}); straight line: Pyruvate entering into TCA cycle (v_7); dashed line: Pyruvate producing alanine (v_{16}). Black: LP with positivity constraint. Red: LP with DMFCA constraints.

6.3 Nucleotides and Biomass Synthesis

Not only nucleotides and biomass fluxes present zero as a feasible solution when DMFCA is applied. Even though a zero flux is mathematically feasible, it is clear from a biological viewpoint that it is not a valid possibility during the cell growth and it would be desirable to have smaller and more realistic intervals for these fluxes. Applying LP to the overdetermined system this problem is apparently resolved. In figure 7, it is observed that both nucleotide

and biomass fluxes achieve the maximum value allowed when DMFCA constraints are imposed. Applying LP with simple positivity constraints, nucleotide flux remains inside the bounded solution found by DMFCA. However the biomass flux presents higher values than the ones computed by DMFCA.

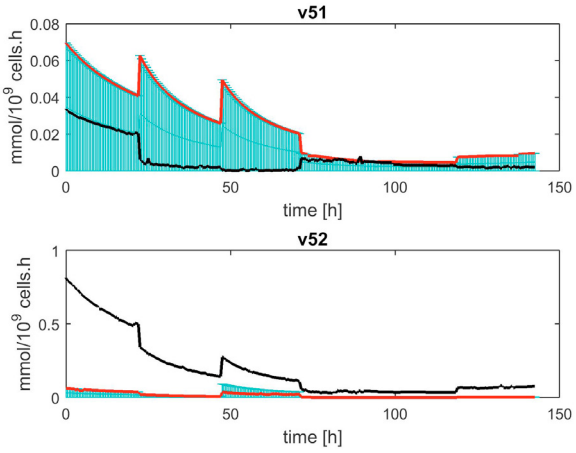

Fig. 7. Dynamic evolution of nucleotides and biomass synthesis along time culture. Turquoise: DMFCA. Black: LP with positivity constraint. Red: LP with DMFCA constraints.

7. CONCLUSIONS

In this study, the dynamic metabolism of fed-batch CHO cell culture is investigated, considering two metabolic networks. The first one is a detailed, underdetermined network, while the second one is a reduced-size network, which is overdetermined. The reduced network belongs to the larger ones, thus allowing a direct comparison.

On the one hand, the underdetermined system is solved by applying dynamic metabolic flux convex analysis, which allows the determination of bounded intervals for the intracellular metabolic fluxes continuously over the culture time. On the other hand, a linear optimization problem is solved to determine the flux distribution in the overdetermined system. This linear optimization problem is solved either imposing simple positivity constraints or box constraints inspired by DMFCA. Considering the underdetermined network as the reference, it is observed in the first problem setting (positivity constraints) that a few fluxes are not contained into the bounded solutions found by DMFCA. This is the case for the flux of pyruvate entering in the TCA cycle (v_7) and biomass synthesis (v_{52}). Nonetheless, most of the fluxes are confined into the bounded solutions found by DMFCA. Imposing box constraints, a feasible solution is found as well by LP. As apparent from the nucleotide (v_{51}) and biomass synthesis (v_{52}), LP with box constraints provides more realistic results than LP with positivity constraints. When the latter is applied, biomass synthesis achieves higher values (even higher than the ones calculated with DMFCA), whereas nucleotides synthesis presents lower values. In contrast, when the former is applied, biomass and nucleotide synthesis present the same trend, which is more realistic from a biological point of view.

ACKNOWLEDGEMENTS

This paper presents research results of the Belgian Network DYSCO (Dynamical Systems, Control, and Optimization), funded by the Interuniversity Attraction Poles Programme initiated by the Belgian Science Policy Office.

REFERENCES

Ahn, W.S. and Antoniewicz, M.R. (2011). Metabolic flux analysis of CHO cells at growth and non-growth phases using isotopic tracers and mass spectrometry. *Metabolic engineering*, 13(5), 598–609.

Fernandes de Sousa, S., Bastin, G., Jolicoeur, M., and Vande Wouwer, A. (2015). Dynamic metabolic flux analysis using a convex analysis approach: Application to hybridoma cell cultures in perfusion. *Biotechnology and bioengineering*.

Leighty, R.W. and Antoniewicz, M.R. (2011). Dynamic metabolic flux analysis (DMFA): a framework for determining fluxes at metabolic non-steady state. *Metabolic engineering*, 13(6), 745–755.

Lequeux, G., Beauprez, J., Maertens, J., Van Horen, E., Soetaert, W., Vandamme, E., and Vanrolleghem, P.A. (2010). Dynamic metabolic flux analysis demonstrated on cultures where the limiting substrate is changed from carbon to nitrogen and vice versa. *BioMed Research International*, 2010.

Llaneras, F., Sala, A., and Picó, J. (2012). Dynamic estimations of metabolic fluxes with constraint-based models and possibility theory. *Journal of Process Control*, 22(10), 1946–1955.

Niklas, J., Schräder, E., Sandig, V., Noll, T., and Heinzle, E. (2011). Quantitative characterization of metabolism and metabolic shifts during growth of the new human cell line AGE1. HN using time resolved metabolic flux analysis. *Bioprocess and biosystems engineering*, 34(5), 533–545.

Pfeiffer, T., Nu, J., Montero, F., Schuster, S., et al. (1999). METATOOL: for studying metabolic networks. *Bioinformatics*, 15(3), 251–257.

Robitaille, J., Chen, J., and Jolicoeur, M. (2015). A Single Dynamic Metabolic Model Can Describe mAb Producing CHO Cell Batch and Fed-Batch Cultures on Different Culture Media. *PloS one*, 10(9), e0136815.

Sengupta, N., Rose, S.T., and Morgan, J.A. (2011). Metabolic flux analysis of CHO cell metabolism in the late non-growth phase. *Biotechnology and bioengineering*, 108(1), 82–92.

Stephanopoulos, G., Aristidou, A.A., and Nielsen, J. (1998). *Metabolic engineering: principles and methodologies*. Academic press.

Terzer, M. and Stelling, J. (2008). Large-scale computation of elementary flux modes with bit pattern trees. *Bioinformatics*, 24(19), 2229–2235.

Vazquez, A., Liu, J., Zhou, Y., and Oltvai, Z.N. (2010). Catabolic efficiency of aerobic glycolysis: the Warburg effect revisited. *BMC systems biology*, 4(1), 58.

Vercammen, D., Logist, F., and Van Impe, J. (2014). Dynamic estimation of specific fluxes in metabolic networks using non-linear dynamic optimization. *BMC systems biology*, 8(1), 132.

Wamelink, M., Struys, E., and Jakobs, C. (2008). The biochemistry, metabolism and inherited defects of the pentose phosphate pathway: a review. *Journal of inherited metabolic disease*, 31(6), 703–717.